Can boron form coordination complexes with diffuse electrons? Evidence for linked solvated electron precursors

To cite this article: Zachary Jordan *et al* 2022 *Electron. Struct.* **4** 015001

Electronic Structure

RECEIVED
28 November 2021

REVISED
20 December 2021

ACCEPTED FOR PUBLICATION
7 January 2022

PUBLISHED
26 January 2022

PAPER

Can boron form coordination complexes with diffuse electrons? Evidence for linked solvated electron precursors

Zachary Jordan, Shahriar N Khan, Benjamin A Jackson and Evangelos Miliordos*

Department of Chemistry and Biochemistry, Auburn University, Auburn, AL 36849-5312, United States of America

* Author to whom any correspondence should be addressed.

E-mail: emiliord@auburn.edu

Keywords: solvated electron, ammonia, hydrogenic shell model, diffuse electrons, excited states

Supplementary material for this article is available online

Abstract

Density functional theory and *ab initio* multi-reference calculations are performed to examine the stability and electronic structure of boron complexes that host diffuse electrons in their periphery. Such complexes (solvated electron precursors or SEPs) have been experimentally identified and studied theoretically for several s- and d-block metals. For the first time, we demonstrate that a p-block metalloid element can form a stable SEP when appropriate ligands are chosen. We show that three ammonia and one methyl ligands can displace two of the three boron valence electrons to a peripheral 1s-type orbital. The shell model for these outer electrons is identical to previous SEP systems (1s, 1p, 1d, 2s). Further, we preformed the first examination of a molecular system consisting of two SEPs bridged by a hydrocarbon chain. The electronic structure of these dimers is very similar to that of traditional diatomic molecules forming bonding and anti-bonding σ and π orbitals. Their ground state electronic structure resembles that of two He atoms, and our results indicate that the excitation energies are nearly independent of the chain length for four carbon atoms or longer. These findings pave the way for the development of novel materials similar to expanded metals and electrides.

1. Introduction

Molecular systems containing one or more diffuse electrons have many applications in redox chemistry, catalysis, and electronics [1]. For both historic and structural reasons, such systems are divided into solutions of solvated electrons, liquid or expanded metals, and electrides (organic and inorganic) [1–26]. These electrons occupy orbitals or bands delocalized around some molecular skeleton. For example, organic electrides are traditionally composed of metal-crown-ether complexes, while expanded metals are made of metal ammonia or methylamine complexes. Experimentally, alkali and alkaline earth metals have been used to synthesize these materials.

Typically, ammonia or crown-ethers stabilize the Li^+, Na^+, K^+, Cs^+, or Ca^{2+} centers and displace the valence electron(s) to the periphery of the complex [27]. These peripheral electrons constitute the electronic bands of the material. Our research group over the past three years has focused on the electronic and geometric structure of metal ammonia complexes with diffuse electrons (dubbed solvated electron precursors (SEPs)) [28–37]. In addition to s-block metals, we have also explored transition metal (d-block) SEPs. The transition metals studied so far (Sc, V, Cr, Y, Mo) adopt formally a 2+ oxidation state with six ammonia ligands in the first coordination sphere; the metal s^2 electrons are displaced to the periphery, residing in the second coordination sphere of the complex [30, 31, 36, 37]. Y and possibly Sc can coordinate eight ammonia molecules and accommodate three peripheral electrons (formerly the metal's s^2d^1 electrons) [30, 36].

The present work targets for the first time the study of a non-metallic (metalloid) p-block element, specifically boron. Our motivation is based on the following questions: can the first coordination sphere of boron

be saturated with ammonia ligands, as in metallic SEPs? Will all three of its valence electrons ($2s^2 2p^1$) be displaced to the outer sphere of the complex? Can ammonia ligands displace a p-type orbital? To answer these questions, we performed high-level quantum chemical calculations combining density functional theory, perturbation theory, and multi-reference wavefunction theory. Our findings indicate that up to three ammonia ligands can coordinate to boron displacing two out of the three valence electrons. A fourth ammonia is not able to coordinate and move the third electron to the periphery. Instead, the addition of a methyl radical results in the formation of a B–C covalent bond and the pseudo-spherical $B(NH_3)_3(CH_3)$ complex with two outer electrons. The effect of replacing CH_3 with NH_2, F, and Cl was also probed. Finally, we connected two $B(NH_3)_3(CH_3)$ entities using a hydrocarbon chain with three to six carbon atoms making a linked-SEP dimer $(NH_3)_m BCH_2(CH_2)_{k-2}CH_2B(NH_3)_n$ [m, n = 0–3 and k = 3–6]. The stability is monitored for all possible combinations of m, n, and k; excited electronic states are examined for the fully saturated monomer and dimers. To our knowledge, this is the first work within the literature to propose or study linked-SEPs. Recent theoretical work has demonstrated SEPs to be effective catalysts in the simultaneous capture and functionalization of CO_2 [38]. The present work is the first demonstration of how SEP centers may be linked and paves the way for the development of novel, redox-active, catalytic materials.

2. Computational details

The geometries of all complexes were optimized with density functional theory. The CAM-B3LYP functional is employed. Previously, this functional has been shown to provide geometries in excellent agreement with MP2 and CCSD(T) for similar systems [35]. The correlation consistent triple-ζ basis sets were chosen for all atoms (cc-pVTZ), and a series of diffuse functions was added on chlorine, fluorine, and hydrogen (aug-cc-pVTZ). The diffuse functions on H are necessary and sufficient for the description of the outer electrons in the ground state of the systems [28]. The energetics (i.e. binding energies) were improved at the MP2 level of theory with the same basis sets. The binding energy D_e for ammonia is calculated using the electronic energies of the molecules before $[M(NH_3)_x]$ and after $[M(NH_3)_{x+1}]$ the addition of ammonia: $D_e = E[M(NH_3)_x] + E[NH_3] - E[M(NH_3)_{x+1}]$. Zero-point energy (ZPE) corrected values are obtained by adding ZPE to the previous energies. ZPE is calculated as 1/2 of the sum of all harmonic vibrational frequencies. The vibrational frequencies are all real for all species and are reported in the supplementary material (SM) (https://stacks.iop.org/EST/4/015001/mmedia).

The reported excitation energies are calculated with CASPT2 (second order perturbation theory applied on a multi-configurational wavefunction—RS2C version of MOLPRO) [39, 40]. The reference calculations are carried out with the state-averaged complete active space self-consistent field (SA-CASSCF) approach. The active space consists of two electrons in ten orbitals for the monomers, and four electrons in eight orbitals for the linked dimers. To keep the calculations manageable for the excited states of linked SEPs, we used the cc-pVDZ basis set for all atoms except for hydrogens, where a d-aug-cc-pVDZ set was used. This approximation has been shown to have little effect in the excitation energies [33, 35], and it is probed presently for the monomers. Also, for technical reasons we applied a shift and IPEA values of 0.2 and 0.25, respectively, to the CASPT2 calculations [31, 41, 42]. The Gaussian16 was invoked to perform the CAM-B3LYP and MP2 calculations [43], while SA-CASSCF and CASPT2 calculations were done with MOLPRO2015 [40]. The IboView software was used to visualize the molecular orbitals [44].

3. Results and discussion

Boron SEP monomers. The ground state of boron has a $1s^2 2s^2 2p^1$ electronic configuration. The approach of three ammonia molecules are able to displace the two 2s electrons from the valence space of boron to the periphery of the ammonia ligands, as happens for $Be(NH_3)_3$ [45]. However, the $2p^1$ electron hinders the attachment of a fourth ammonia, which prefers to populate the second solvation shell of $B(NH_3)_3$. We were actually able to locate a $B(NH_3)_4$ structure with all three valence boron electrons displaced in the periphery of the complex, but is metastable (higher in energy with respect to $B(NH_3)_3 + NH_3$) by 20 kcal mol^{-1} (18 kcal mol^{-1} after ZPE corrections). The potential energy curves for the approach of the fourth ammonia ligand is revealing and are reported in figure S1 of the SM. There is a large activation energy barrier ($\sim$40 kcal mol^{-1}) and the products of the 'reaction' are higher than the 'reactants'. The reason can be ascribed to the metalloid (and not metallic) nature of boron as demonstrated by its large third ionization energy (37.9 eV) [46] compared to that of metallic aluminum in the same group of the periodic table (28.4 eV) [46]. The occupation of the 2p orbital effectively repels the approach of a fourth ammonia while the large ionization energy prevents its displacement to the periphery.

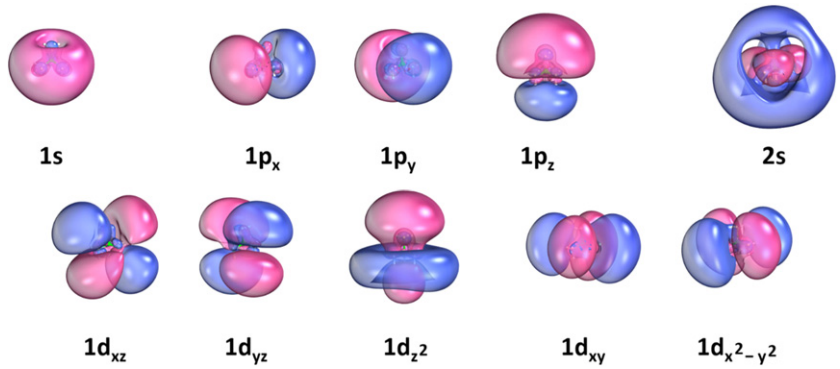

Figure 1. Molecular outer orbitals of $CH_3B(NH_3)_3$.

Table 1. MP2 plain and ZPE corrected (D_e/D_0) binding energies of CAM-B3LYP optimized, substituted boron ammonia monomers $XB(NH_3)_n$ in kcal mol^{-1}.

n	$X = F$	$X = Cl$	$X = NH_2$	$X = CH_3$
0[a]	186.3/184.3	123.2/122.0	134.0/130.1	93.0/89.7
1[b]	−10.2/−12.8	8.6/5.7	10.1/5.3	12.3/8.6
2[b]	13.4/9.4	16.9/12.4	1.8/−0.9	22.1/18.0
3[b]	6.4/4.5	−0.8/−2.0	7.8/5.2	8.0/6.3

[a]The binding energies on this line refer to the BX (ground $S = 0$ state) → B (^{2}P; $2s^2 2p^1$) + X (ground $S = 1/_2$ state) dissociation.
[b]The binding energies on these lines refer to the $XB(NH_3)_n$ (ground $S = 0$ state) → $XB(NH_3)_{n-1}$ (ground $S = 0$ state) + NH_3 ($^1A_1$) dissociation.

The saturation of the first coordination sphere of boron can be achieved by using the $2p^1$ electron to form a covalent bond or ionic bond with a ligand such as fluorine, chlorine, NH_2 or CH_3. Indeed, the potential energy curves for the approach of CH_3 are smooth leading to a stable product (compare figures S1 and S2 of SM). The proposed $XB(NH_3)_3$ (X = F, Cl, NH_2, CH_3) complexes have a pseudospherical geometry, especially for $X = CH_3$, and can accommodate two peripheral electrons. The orbitals hosting these two electrons are shown in figure 1 for $CH_3B(NH_3)_3$. These include the lowest energy 1s outer orbital, followed by three 1p, five 1d, and one 2s orbitals. The methyl group, which sits on the top side of the molecule in figure 1, creates some anisotropy to the system destabilizing orbitals with components along the z-direction, e.g. $1p_z$ and $1d_z{}^2$.

The ground state for all $XB(NH_3)_3$ species has a $1s^2$ configuration. The optimal geometries and harmonic frequencies are reported in the SM section. The binding energy of the X unit is as large as 186.3 kcal mol^{-1} for X = F (see table 1) decreasing to 134.0 kcal mol^{-1} for $X = NH_2$, 123.2 kcal mol^{-1} for X = Cl, and as small as 93.0 kcal mol^{-1} for $X = CH_3$. All are very strong as compared to the subsequent B–NH_3 bonds. The D_e value for the first ammonia is of the order of 10 kcal mol^{-1} for all systems except for X = F, where it is negative. The second ammonia binds more strongly for all species except $X = NH_2$, and the third ammonia is metastable for X = Cl. The $CH_3B(NH_3)_3$ complex is the only system with all three ammonia ligands having positive D_e and D_0 values (see table 1). The first ammonia binds with 12.3 kcal mol^{-1} energy, the second with 22.1 kcal mol^{-1}, and the third with 8.0 kcal mol^{-1}. The average D_e value of 14.1 kcal mol^{-1} is comparable to the $Be(NH_3)_3$ value of 12.8 kcal mol^{-1} [45], and that of $Li(NH_3)_4$ (13.6 kcal mol^{-1}; present MP2 calculations). $Li(NH_3)_4$ has only one outer electron and has been identified experimentally [47].

The low-lying electronic states of the $XB(NH_3)_3$ species are listed in table 2. More complete data are provided in the SM. The first excited state is a triplet with one 1s electron being promoted to one of the three 1p orbitals. The $1s^1 1p_{x,y}{}^1$ states are nearly degenerate in every case and about 0.2 eV lower in energy than $1s^1 1p_z{}^1$. Table 2 lists the energy range for all three states (0.8–1.2 eV with triple-ζ basis set). Notice that $1p_z$ is polarized toward X as opposed to 1s, which is polarized to the opposite direction. The singlet $1s^1 1p^1$ states are next (1.5–2.0 eV) following the same pattern with $1s^1 1p_{x,y}{}^1$ being lower than $1s^1 1p_z{}^1$ by a slightly larger amount (0.3–0.4 eV). The excitation energies for both singlet and triplet $1s^1 1p^1$ states is nearly independent of the X unit within 0.1–0.2 eV. The next states are a group of singlet states (1.8–2.3 eV) with $1s^1 1d^1/1p^2$ mixed character ($1s^1 \rightarrow 1d^1$ or $1s^2 \rightarrow 1p^2$ excitations) followed by the $1s^1 1d^1$ triplet states. The mingling of $1p^2$ configurations with the $1s^1 1d^1$ singlet spin states stabilize them over the $1s^1 1d^1$ triplet states, which lie at 2.0–2.5 eV. This is the opposite of what happens for the $1s^1 p^1$ states. The next electronic states are generally

Table 2. Electronic configurations (Config.), spin (S), and CASPT2 excitation energies or energy ranges for $XB(NH_3)_3$, X = F, Cl, NH_2, CH_3, and $Be(NH_3)_4$ using double-ζ (DZ)[a] or triple-ζ (TZ)[b] basis sets.

Config.	S	X = F	X = Cl	X = NH_2[c]	X = CH_3[c]	$Be(NH_3)_4$[c,d]
			Basis set = DZ			
$1s^2$	0	0.000	0.000	0.000	0.000	
$1s^1 1p^1$	1	0.826–1.161	0.853–1.112	0.740–1.087	0.776–1.072	
$1s^1 1p^1$	0	1.605–2.044	1.649–2.018	1.518–1.875	1.563–1.869	
$1s^1 1d^1/1p^2$	0	1.877–2.321	1.875–2.291	1.810–2.180	1.734–2.129	
$1s^1 1d^1$	1	2.088–2.467	2.052–2.486	1.917–2.358	1.936–2.310	
$1s^1 2s^1$	1	2.401	2.417	2.355	2.283	
$1s^1 2s^1$	0	2.551	2.514	2.464	2.427	
			Basis set = TZ			
$1s^2$	0	0.000	0.000	0.000	0.000	0.00
$1s^1 1p^1$	1	0.844–1.161	0.871–1.105	0.756–1.096	0.792–1.075	0.81
$1s^1 1p^1$	0	1.617–2.079	1.658–2.042	1.528–1.909	1.576–1.893	1.62
$1s^1 1d^1/1p^2$	0	1.908–2.343	1.903–2.338	1.838–2.202	1.762–2.146	1.65–1.82
$1s^1 1d^1$	1	2.106–2.485	2.068–2.491	1.986–2.385	1.948–2.320	1.93–2.11
$1s^1 2s^1$	1	2.432	2.453	2.391	2.300	2.24
$1s^1 2s^1$	0	2.571	2.529	2.484	2.440	2.30

[a]DZ = cc-pVDZ (B, N, C), aug-cc-pVDZ (F, Cl), and d-aug-cc-pVDZ (H).
[b]TZ = cc-pVTZ (B, N, C), aug-cc-pVTZ (F, Cl), and d-aug-cc-pVTZ (H).
[c]These molecules have additional multi-reference states between the triplet $1s^1 1d^1$ and the $1s^1 2s^1$ states. Some of them are of impure nature.
[d]Reference [28]; CASPT2/TZ.

of multi-reference character and are provided in the SM. We singled out the triplet and singlet $1s^1 2s^1$ states at ∼2.5 eV. The triplet state is lower again by 0.4–0.7 eV (see table 2).

Another comment is that the double-ζ quality excitation energies listed in table 2 are in remarkable agreement with the triple-ζ quality. This means that the double-augmentation scheme on each hydrogen center provides an adequately large number of basis functions to describe the diffuse nature of the outer electrons independently of the cardinal number of the used correlation-consistent basis set. Finally, we compare the excitation energies with those of the more symmetric (tetrahedral) $Be(NH_3)_4$ using the triple-ζ basis sets; see table 2 and reference [28]. For $Be(NH_3)_4$ the 1p orbitals are exactly degenerate, while the 1d orbitals stay within a smaller energy range due to the higher symmetry. In every case, the excitation energies of $Be(NH_3)_4$ are within the energy range of the electronic energies of $CH_3Be(NH_3)_3$.

Linked boron SEP monomers. Given the higher stability of $CH_3B(NH_3)_3$ over the other $XB(NH_3)_4$ species, we considered the linkage of two $CH_3B(NH_3)_3$ monomers via an aliphatic hydrocarbon bridge. In this section, we investigate the stability and structure of $(NH_3)_nB(CH_2)_kB(NH_3)_m$ for k = 3–6 and m, n = 1–3, and excited states of the fully coordinated $(NH_3)_3B(CH_2)_{3-6}B(NH_3)_3$ species. Smaller carbon chains led to the formation of species with B–B bonds, which are not of our interest in this study.

Figure 2 shows the structure of the species we considered for $k = 4$. Similar structures are considered for other k values. The top structure contains no ammonia ligands and the second has one ammonia ligand at one of the boron terminals. The next three rows correspond to systems with two ($m + n = 2$), three ($m + n = 3$), and four ($m + n = 4$) ammonia ligands. Each has two isomers varying how many ammonia ligands are on each terminus. For example, the two ammonia ligands can be both on one side or can attach to different boron terminals, i.e. $(m, n) = (2, 0)$ or $(0, 2)$ or $(1, 1)$. Similarly for $m + n = 3$ we have $(m, n) = (3, 0)$ or $(0, 3)$ or $(1, 2)$ or $(2, 1)$, and for $m + n = 4$ we have $(m, n) = (3, 1)$ or $(1, 3)$ or $(2, 2)$. As indicated in figure 2, the first two ammonias bind to the same boron atom, while the third and fourth prefer to bind to the other boron atom. This trend can be rationalized by looking at the binding energies for the $CH_3B(NH_3)_{1-3}$ systems of table 1. The binding energy of the third ammonia ligand to the same boron center is smaller than the binding energies for the attachment of the first two ammonia ligands. Therefore, the third and fourth ammonias prefer to bind to the second boron atom of the dimeric species. In addition, the first ammonia ligand attaches to boron always in the eclipsed position relative to the carbon chain.

Table 3 tabulates the binding energies for all ammonia ligands. The lowest energy isomer is always considered. The binding energy values are very close to those found for the monomer species (compare values below with values from table 1). Depending on the size of the carbon chain, the first ligand of each boron binds with 14.3–15.7 kcal mol^{-1} ($n + m = 1$) or 13.2–13.7 kcal mol^{-1} ($m + n = 3$). The second ligand binds with 22.2–22.5 kcal mol^{-1} ($n + m = 2$) or 21.6–22.0 kcal mol^{-1} ($n + m = 4$), and the third one by 4.6–5.1 kcal mol^{-1} ($n + m = 5$) or 4.9–5.6 kcal mol^{-1} ($n + m = 6$). Therefore, the carbon chain size minimally affects the stability of the two linked boron monomers. Table 3 also lists the energy difference for the two isomers for $m + n = 2$, 3, 4. In the first two cases, the lowest energy isomer is more stable by

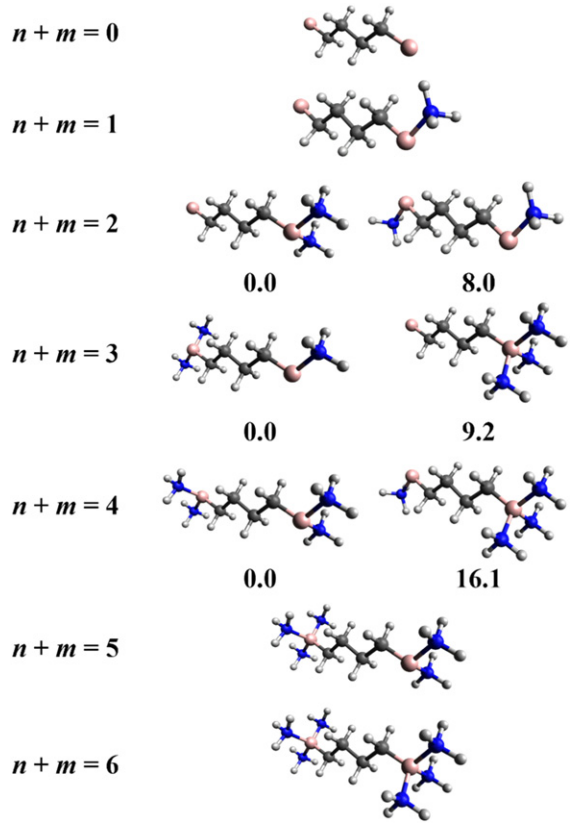

Figure 2. CAM-B3LYP global minima for $(NH_3)_nB(CH_2)_4B(NH_3)_m$. Relative energies in kcal mol^{-1} are reported for the two possible isomers with $n + m = 2$, 3, and 4.

Table 3. MP2//CAM-B3LYP binding energies (D_e) for the lowest energy isomers and energy difference between the two lowest energy isomers (ΔE) of $(NH_3)_nB(CH_2)_kB(NH_3)_m$ in kcal mol^{-1}.

$n+m$		$k=3$	$k=4$	$k=5$	$k=6$
1	D_e	15.7	14.9	14.5	14.3
2	D_e	22.5	22.2	22.4	22.2
	ΔE[a]	9.1	8.0	8.5	8.0
3	D_e	13.7	13.2	13.5	13.5
	ΔE[b]	10.2	9.2	9.2	8.9
4	D_e	22.0	21.6	21.7	21.6
	ΔE[c]	16.7	16.1	16.4	16.4
5	D_e	4.6	5.4	5.0	5.1
6	D_e	5.6	5.0	5.0	4.9

[a]The $n = 2$, $m = 0$ isomer is higher in energy.
[b]The $n = 2$, $m = 1$ isomer is higher in energy.
[c]The $n = 3$, $m = 1$ isomer is higher in energy.

9.1 $\pm$ 1.1 kcal mol^{-1}; however, for $m + n = 4$, the isomers differ by 16.4 $\pm$ 0.3 kcal mol^{-1} as the higher energy isomer involves the attachment of a third ammonia to the same boron atom.

We now turn our discussion to the fully coordinated $(NH_3)_3B(CH_2)_{3-6}B(NH_3)_3$ species. Based on the electronic structure of $(NH_3)_3BCH_3$ (*see above*), the ground state of the dimer should have two electrons in the periphery of each boron side. Due to symmetry, the two outer 1s orbitals of each side are combined with an in-phase or out-of-phase interaction to make a 'bonding' and an 'anti-bonding' combination (orbitals σ_s and σ_s^* of figure 3). Therefore, the ground state of the dimeric species has a $\sigma_s^2\sigma_s^{*2}$ electronic configuration. This electronic structure resembles that of two bonded He atoms. Under standard conditions, the He_2 is practically unstable with an equilibrium distance of 3.0 Å and an interaction energy of 11 K or 7.6 cm^{-1} [48]. In contrast, the aliphatic linkage of the boron SEPs produces a highly-stable dimeric system.

The resemblance of the studied species with traditional diatomic molecules is further demonstrated by the orbitals populated in the excited states. Specifically, the next available orbitals are of π/π^* and σ/σ^* character and made of the 1p orbitals of the two monomers (see figure 3). Identical behavior was seen for the $[Li(NH_3)_4]_2$

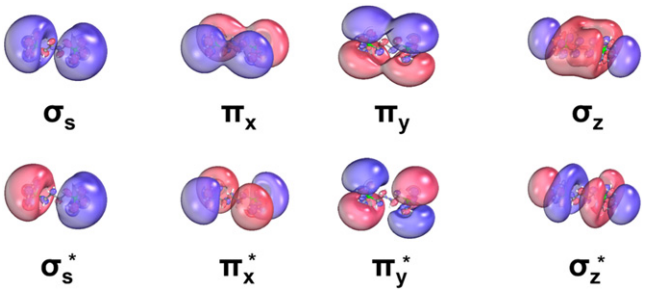

Figure 3. Molecular outer orbitals of $(NH_3)_3B(CH_2)_4B(NH_3)_3$.

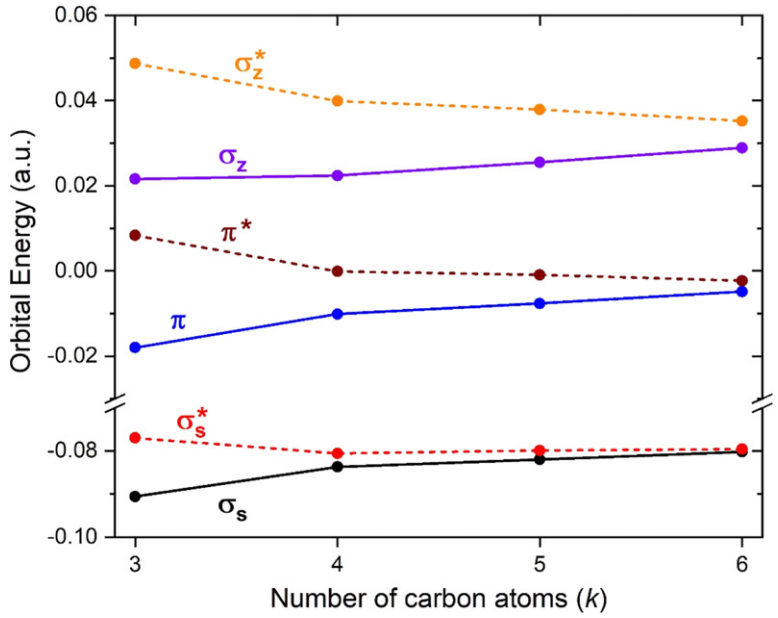

Figure 4. Energy of the $(NH_3)_3B(CH_2)_kB(NH_3)_3$, $k = 3$–6, molecular outer orbitals as a function of the carbon chain size at SA-CASSCF.

dimers [29], which are not connected via a hydrocarbon bridge but are bound via a σ-bond of the two outer 1s electrons of each $Li(NH_3)_4$ complex. As expected, σ_s is followed σ_s^* and their energy converges to degeneracy for longer carbon chains. Figure 4 shows the energy dependence of these outer orbitals (SA-CASSCF) as a function of the carbon chain length. The two π or π^* orbitals are degenerate within 0.006 a.u. for $k = 3$ and 0.0005 a.u. for $k = 6$. Unlike traditional diatomic molecules, the next orbital is not σ_z but the π followed by π^*. The reason is that the 'bonding' density of σ_z is around the carbon chain, a rather unfavorable region for the electrons (C–H bonds are not generally involved in solvating electrons). Again, π/π^* and σ_z/σ_z^* orbitals converge to the same value for longer chains as expected due to larger separation of the two monomers and thus smaller overlap between their 'atomic' outer orbitals.

The first four excited states lie within <0.1 eV from each other and around 0.75 eV from the ground state for all k values (see table 4). These triplet states are generated when one electron moves from either σ_s or σ_s^* to either a π or π^* orbital. The next two states at 1.1–1.2 eV are formed by the promotion of one σ_s or σ_s^* electron to the σ_z or σ_z^* orbitals, also of triplet spin multiplicity. The next state is a quintet state at 1.26 eV ($k = 3$) and 1.52 ± 0.03 eV for $k > 3$, when one σ_s and one σ_s^* electrons migrate to the π/π^* orbitals. Up to 1.6 eV, 11 electronic states were found of singlet, triplet, and quintuple spin multiplicity, with half of them being highly multi-configurational states. Table 4 lists the electronic configurations for the single reference states and the excitation energies for all states.

Table 4. Electronic configurations (Config.), spin (S), and CASPT2 vertical excitation energies (eV) for the low-lying electronic states of $(NH_3)_3B(CH_2)_kB(NH_3)_3$, $k = 3$–6[a].

Config.	S	$k = 3$	$k = 4$	$k = 5$	$k = 6$
$\sigma_s^2\sigma_s^{*2}$	0	0.00	0.00	0.00	0.00
$\sigma_s^2\sigma_s^{*1}\pi_x^1 - \sigma_s^1\sigma_s^{*2}\pi_y^1$	1	0.69	0.74	0.74	0.74
$\sigma_s^2\sigma_s^{*1}\pi_y^{*1} + \sigma_s^1\sigma_s^{*2}\pi_x^{*1}$	1	0.72	0.78	0.77	0.77
$\sigma_s^2\sigma_s^{*1}\pi_y^1 + \sigma_s^1\sigma_s^{*2}\pi_x^1$	1	0.75	0.74	0.74	0.74
$\sigma_s^2\sigma_s^{*1}\pi_x^{*1} - \sigma_s^1\sigma_s^{*2}\pi_y^{*1}$	1	0.76	0.76	0.76	0.76
$\sigma_s^2\sigma_s^{*1}\sigma_z^1 + \sigma_s^1\sigma_s^{*2}\sigma_z^{*1}$	1	1.14	1.17	1.17	1.17
$\sigma_s^2\sigma_s^{*1}\sigma_z^{*1} - \sigma_s^1\sigma_s^{*2}\sigma_z^1$	1	1.16	1.15	1.15	1.15
$\sigma_s^1\sigma_s^{*1}\left(\pi_x^1\pi_y^{*1} + \pi_x^{*1}\pi_y^1\right)$	2	1.26	1.54	1.49	1.51
MR[b]	1	1.35	1.52	1.49	1.50
MR[b]	0	1.37	1.53	1.50	1.51
MR[b]	0	1.43	1.51	1.51	1.51
MR[b]	1	1.47	1.50	1.51	1.50
$\sigma_s^1\sigma_s^{*1}\left(\pi_x^2 - \pi_y^2\right)$	0	1.49	1.49	1.48	1.47
$\sigma_s^1\sigma_s^{*1}\left(\pi_x^*2 - \pi_y^{*2}\right)$	0	1.50	1.55	1.55	1.54
MR[b]	1	1.52	1.50	1.49	1.48
MR[b]	1	1.54	1.56	1.55	1.54
$\sigma_s^1\sigma_s^{*1}\left(\pi_x^1\pi_x^{*1} - \pi_y^{*1}\pi_y^1\right)$	2	1.55	1.49	1.52	1.51
$\sigma_s^1\sigma_s^{*1}\pi_x^1\pi_y^1$	2	1.56	1.51	1.49	1.48
$\sigma_s^1\sigma_s^{*1}\pi_x^{*1}\pi_y^{*1}$	2	1.61	1.57	1.56	1.55

[a]DZ = cc-pVDZ (B, N, C)/d-aug-cc-pVDZ (H).
[b]Highly multi-reference states involving multiple excitations from σ_s and σ_s^* orbitals to π and π^* orbitals.

4. Summary and conclusions

High-level quantum chemical calculations are used to study the stability and electronic structure of boron-SEPs. Boron can make stable, fully coordinated (saturated) complexes with two diffuse outer electrons by attaching three ammonia ligands and one methyl radical. The outer electrons of the formed pseudo-spherical molecular system reside in a hydrogenic-type shell model, resembling the isovalent $Be(NH_3)_4$ complex. The first four orbitals follow the same 1s, 1p, 1d, 2s order observed for other s- and d-block metal SEPs. The excited states of $CH_3B(NH_3)_3$ possess the same pattern (in terms of electronic configurations and excitation energies) as $Be(NH_3)_4$ confirming that the 'behavior' of the outer electrons is practically independent of the nature of the central metal [37]. For the first time, we also showed that a hydrocarbon chain can bridge two SEPs and create an analogue of a diatomic molecule (linked SEP). The atomic-type diffuse orbitals 1s and 1p of each boron SEP monomer are combined to produce σ, σ^*, π, π^*-type orbitals. The effect of the chain length on excitation energies for states involving these orbitals is minimal for chains of four carbons and longer. Our findings are expected to guide future experimental studies toward the discovery of new materials similar to expanded metals.

Acknowledgments

The authors are indebted to Auburn University (AU) for financial support. EM is especially grateful to the donors of the James E Land endowment. This work was completed with resources provided by the Auburn University Easley Cluster. This material is based upon work supported by the National Science Foundation under Grant No. CHE-1940456. Any opinions, findings, and conclusions or recommendations expressed in this material are those of the author(s) and do not necessarily reflect the views of the National Science Foundation.

Data availability statement

All data that support the findings of this study are included within the article (and any supplementary files).

Supplementary material

The supporting information lists detailed information on the excited states, the geometries/frequencies/energies of the ground states for all species studied presently.

References

[1] Zhang X and Yang G 2020 *J. Phys. Chem. Lett.* **11** 3841–52
[2] Ellaboudy A, Dye J L and Smith P B 1983 *J. Am. Chem. Soc.* **105** 6490–1
[3] Dawes S B, Ward D L, Huang R H and Dye J L 1986 *J. Am. Chem. Soc.* **108** 3534–5
[4] Huang R H, Faber M K, Moeggenborg K J, Ward D L and Dye J L 1988 *Nature* **331** 599–601
[5] Wagner M J, Huang R H, Eglin J L and Dye J L 1994 *Nature* **368** 726–9
[6] Huang R H, Wagner M J, Gilbert D J, Reidy-Cedergren K A, Ward D L, Faber M K and Dye J L 1997 *J. Am. Chem. Soc.* **119** 3765–72
[7] Xie Q, Huang R H, Ichimura A S, Phillips R C, Pratt W P and Dye J L 2000 *J. Am. Chem. Soc.* **122** 6971–8
[8] Dye J L 2003 *Science* **301** 607
[9] Redko M Y, Jackson J E, Huang R H and Dye J L 2005 *J. Am. Chem. Soc.* **127** 12416–22
[10] Toda Y, Kubota Y, Hirano M, Hirayama H and Hosono H 2011 *ACS Nano* **5** 1907–14
[11] Lee K, Kim S W, Toda Y, Matsuishi S and Hosono H 2013 *Nature* **494** 336–40
[12] Liu C, Nikolaev S A, Ren W and Burton L A 2020 *J. Mater. Chem.* C **8** 10551–67
[13] Ammari Y and Hlil E K 2021 *Chem. Pap.* **75** 3197
[14] Yang X, Parrish K, Li Y-L, Sa B, Zhan H and Zhu Q 2021 *Phys. Rev.* B **103** 125103
[15] Edwards P P, Lusis A R and Sienko M J 1980 *J. Chem. Phys.* **72** 3103–12
[16] Hagedorn R and Sienko M J 1982 *J. Phys. Chem.* **86** 2094–7
[17] Stacy A M, Johnson D C and Sienko M J 1982 *J. Chem. Phys.* **76** 4248–54
[18] Stacy A M and Sienko M J 1982 *Inorg. Chem.* **21** 2294–7
[19] Nakamura Y, Niibe M and Shimoji M 1984 *J. Phys. Chem.* **88** 3755–60
[20] Kohanoff J, Buda F, Parrinello M and Klein M L 1994 *Phys. Rev. Lett.* **73** 3133–6
[21] Hayama S, Wasse J C, Skipper N T and Soper A K 2002 *J. Phys. Chem* B **106** 11–4
[22] Thompson H, Wasse J C, Skipper N T, Hayama S, Bowron D T and Soper A K 2003 *J. Am. Chem. Soc.* **125** 2572–81
[23] Ibberson R M, Fowkes A J, Rosseinsky M J, David W I F and Edwards P P 2009 *Angew. Chem., Int. Ed.* **48** 1435–8
[24] Maeda K, Lodge M T J, Harmer J, Freed J H and Edwards P P 2012 *J. Am. Chem. Soc.* **134** 9209–18
[25] Seel A G, Swan H, Bowron D T, Wasse J C, Weller T, Edwards P P, Howard C A and Skipper N T 2017 *Angew. Chem., Int. Ed.* **56** 1561–5
[26] Mauksch M and Tsogoeva S B 2018 *Phys. Chem. Chem. Phys.* **20** 27740–4
[27] Ariyarathna I R and Miliordos E 2021 *Phys. Chem. Chem. Phys.* **23** 20298–306
[28] Ariyarathna I R, Khan S N, Pawłowski F, Ortiz J V and Miliordos E 2018 *J. Phys. Chem. Lett.* **9** 84–8
[29] Ariyarathna I R, Pawłowski F, Ortiz J V and Miliordos E 2018 *Phys. Chem. Chem. Phys.* **20** 24186–91
[30] Almeida N M S and Miliordos E 2019 *Phys. Chem. Chem. Phys.* **21** 7098–104
[31] Almeida N M S, Pawłowski F, Ortiz J V and Miliordos E 2019 *Phys. Chem. Chem. Phys.* **21** 7090–7
[32] Ariyarathna I R, Almeida N M S and Miliordos E 2019 *J. Phys. Chem* A **123** 6744–50
[33] Ariyarathna I R and Miliordos E 2019 *Phys. Chem. Chem. Phys.* **21** 15861–70
[34] Ariyarathna I R and Miliordos E 2020 *J. Phys. Chem* A **124** 9783–92
[35] Ariyarathna I R, Pawłowski F, Ortiz J V and Miliordos E 2020 *J. Phys. Chem* A **124** 505–12
[36] Khan S N and Miliordos E 2020 *J. Phys. Chem* A **124** 4400–12
[37] Jackson B A and Miliordos E 2021 *J. Chem. Phys.* **155** 014303
[38] Jackson B A and Miliordos E Chem. *Commun.* accepted https://doi.org/10.1039/D1CC04748E
[39] Celani P and Werner H-J 2000 *J. Chem. Phys.* **112** 5546–57
[40] Werner H-J *et al* 2015 *MOLPRO version 2015.1,* a package of ab initio programs
[41] Roos B O and Andersson K 1995 *Chem. Phys. Lett.* **245** 215–23
[42] Ghigo G, Roos B O and Malmqvist P-Å 2004 *Chem. Phys. Lett.* **396** 142–9
[43] Frisch M J *et al* 2016 *Gaussian 16 Rev. C.01* (Wallingford CT: Gaussian, Inc.)
[44] Knizia G 2019 *IboView* (http://iboview.org/) (accessed 15 December 2019)
[45] Ariyarathna I R and Miliordos E 2018 *Int. J. Quantum Chem.* **118** e25673
[46] Haynes W M 2012 *CRC Handbook of Chemistry and Physics* 93rd edn (London: Taylor and Francis)
[47] Takasu R, Misaizu F, Hashimoto K and Fuke K 1997 *J. Phys. Chem* A **101** 3078–87
[48] Jeziorska M, Cencek W, Patkowski K, Jeziorski B and Szalewicz K 2007 *J. Chem. Phys.* **127** 124303